

The corresponding inertial velocity error (or deviation) referred to the rotating coordinate system is given by

$$\Delta \dot{\mathbf{r}}^* \equiv \begin{bmatrix} \Delta \dot{x}^* \\ \Delta \dot{y}^* \\ \Delta \dot{z}^* \end{bmatrix} = \begin{bmatrix} \Delta \dot{x} + n^*(p^2/r^2) \Delta z \\ \Delta \dot{y} \\ \Delta \dot{z} - n^*(p^2/r^2) \Delta x \end{bmatrix} \quad (4)$$

Solving Eqs (3) and (4) as an initial value problem will yield the "transition" matrix, which is the desired solution as given in Table 1. It is needless to state here that the derivation for this solution is complex inasmuch as the differential equations involve time-varying coefficients. An exact integral to Eq (3) has been obtained but will not be given here for lack of space.

For circular orbits $p/r = 1$, and Eqs (3) and (4) become constant coefficient equations which can be directly solved as an initial value problem using Laplace Transform techniques. This solution is given in Refs 1-5.

Let the matrix solution of Table 1 be denoted by ϕ and assume that it is partitioned as a set of four 3×3 submatrices. Then the solution to Eq (3) can be represented as

$$\begin{bmatrix} \Delta \mathbf{r}_{n+1} \\ \Delta \dot{\mathbf{r}}_{n+1}^* \end{bmatrix} = \begin{bmatrix} \alpha_{n+1} & \beta_{n+1} \\ \dot{\alpha}_{n+1} & \dot{\beta}_{n+1} \end{bmatrix} \begin{bmatrix} \Delta \mathbf{r}_n \\ \Delta \dot{\mathbf{r}}_n^* \end{bmatrix} \quad (5)$$

in which this matrix, defined as $\phi_{n+1, n}$, is given by Table 1, and where, typically, $\alpha_{n+1, n} = \alpha(t_{n+1}, t_n)$ is a 3×3 submatrix evaluated between the two terminals $n+1$ and n . The inertial position and velocity deviation propagation and error equations are then given by Eq (5). To obtain the inverse (lower matrix of Table 1), use can be made of the relationship

$$\phi^{-1} = \begin{bmatrix} \beta^T & -\dot{\beta}^T \\ -\dot{\alpha}^T & \alpha^T \end{bmatrix} \quad (6)$$

which is proved in Ref 8 for inertial coordinates systems and in Refs 6 and 7 for rotating coordinate systems.

An Explicit Linear Guidance Law

Using Eq (5), a linear deterministic solution to the two-point boundary problem that involves impulsive controls can be developed. In most linear guidance schemes in the free-fall regime, it is desired to secure a position and/or velocity match at a future epoch. This implies one velocity correction to null the predicted position deviation and a second correction to null the velocity deviation. The velocity-to-be-gained to null the predicted position deviation at epoch $n+1$ is given as

$$\Delta \mathbf{v}_n^1 = -[\beta_{n+1, n}^{-1} \alpha_{n+1, n}][I] \begin{bmatrix} \Delta \mathbf{r}_n \\ \Delta \dot{\mathbf{r}}_n^* \end{bmatrix} \quad (7)$$

The velocity-to-be-gained to be applied at $n+1$ to null the velocity deviation at $n+1$ is given by

$$\Delta_{n+1} \mathbf{v}^2 = (\beta_{n+1, n}^{-1})^T \Delta \mathbf{r}_n \quad (8)$$

Further details on linear impulsive guidance mechanization techniques are given in Ref 7. The previously cited Table 2 yields the explicit representation of the velocity-to-be-gained sensitivity matrixes, $-\beta^{-1}\alpha$ and $[\beta^{-1}]^T$, for all two-body conical orbits.

References

- 1 Clohessy, W. H. and Wiltshire, R. S., "Terminal guidance system for satellite rendezvous," *J. Aerospace Sci.* 27, 653-658 (1960).
- 2 Eggleston, J. M. and Dunning, R. S., "Analytical evaluation of a method of midcourse guidance for rendezvous with earth satellites," NASA TN D-883 (October 1962).
- 3 Hord, R. A., "Relative motion in the terminal phase of interception of a satellite or ballistic missile," NASA TN 4399 (1958).
- 4 Wheelon, A. D., "Midcourse and terminal guidance," *Space Technology* (John Wiley and Sons, Inc., New York, 1959), Chap 26.
- 5 Kochi, K. C., "An introduction to midcourse navigation-guidance," Autonetics Rept. EM 262-265 (October 1962).

⁶ Kochi, K. C., "Navigation-guidance mechanization equations for two-body orbits," Autonetics Tech. Memo 243-2-150 (May 1963).

⁷ Kochi, K. C., "A 'universal' linear guidance mechanization for space systems," Autonetics Tech. Memo 243-2-153 (June 1963).

⁸ McLean, J. D., Schmidt, S. F., and McGee, L. A., "Optimal filtering and linear prediction applied to a midcourse navigation system for circumlunar missions," NASA TN D-1208 (1962).

Mars Nonstop Round-Trip Trajectories

ROGER W. LUIDENS*

NASA Lewis Research Center, Cleveland, Ohio

Introduction

MANNED and unmanned nonstop round trips may be precursors of the first manned landing on Mars. The vehicle for such a trip will be launched from Earth and, without stopping, fly by Mars and return to Earth. Except in special cases, a vehicle placed on a trajectory to Mars will not return to Earth. In many cases, however, an Earth return can be achieved if the trajectory is modified by one of the following means: 1) by the gravity of Mars, 2) by gravity supplemented by propulsion, or 3) by gravity supplemented by aerodynamic forces. The analysis of the trajectories resulting from the latter two trajectory modifications is the contribution made herein.

In this note, the preceding three kinds of nonstop round trip trajectories are compared in the years 1971 and 1980 on the basis of mission time and the required propulsive velocity increment. A short mission is desirable for reducing life support system weight and for psychological reasons. Since the initial system gross weight is exponentially related to the propulsive velocity increment, a low value of this parameter also is desired.

Types of Maneuvers

The trajectory of a typical nonstop round-trip mission in 1971 is superimposed on orbits of Mars and Earth in Fig. 1. Note that the Mars orbit is quite eccentric. The vehicle leaves Earth at point 1, passes close to Mars at point 2, and returns to Earth at point 3. In general, outbound and inbound legs of the trajectory are of unequal length.

When the vehicle passes Mars, its trajectory can be changed in three ways, which characterize the three trajectories analyzed (Fig. 2). For a gravity turn, only the gravitational field of Mars deflects the vehicle (Fig. 2a). The arrival and the departure velocities V_A and V_D are equal in magnitude, and the turning is equally distributed between the arrival and the departure phases of the maneuver, that is, $\Phi_{GA} = \Phi_{GD}$.

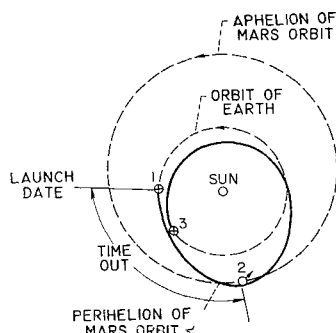
If gravity alone cannot produce an Earth return trajectory, the trajectory can be further changed by thrusting. The thrust is generally best applied at the sphere of influence when the vehicle departs from Mars. Figure 2a illustrates a velocity increment ΔV_G imparted to change the departure velocity vector from V_D to V_D' . A trajectory using this maneuver is called a propulsive-gravity turn.

An aerodynamic-turn trajectory (Fig. 2b) may be used to advantage when a low departure velocity and a high turning angle are required. The total turning can be broken into three stages. First, the arrival velocity vector is turned through an angle Φ_{GA} by the planetary gravitation field. Second, after entering the Mars atmosphere, the vehicle

Received October 17, 1963. The author wishes to acknowledge the assistance of Jay M. Kappaff and Richard J. Flaherty in conducting the present analysis.

* Head, Flight Systems Section, Mission Analysis Branch, Associate Fellow Member AIAA.

Fig 1 Mars nonstop round-trip trajectory in 1971



velocity vector is turned through an angle Φ_α by the vehicle lift and is also decreased in magnitude because of aerodynamic drag. Finally, after the vehicle leaves the Mars atmosphere and until it departs from the sphere of influence of Mars, it is turned through an angle Φ_{GD} .

Method of Analysis

The round-trip trajectories were studied by first selecting the type of nonstop trajectory, the launch year, and the total trip time (equivalent to the central angle from 1 to 3 in Fig 1). Then, by varying the launch date and the time out, the trajectories with a minimum propulsive velocity increment were located. The trajectory data were generated by the "patch-conic, impulsive ΔV " computer program of Ref 1, which accounts for both the eccentricity and the inclinations of the Earth and the Mars orbits.

Results and Discussion

The minimum propulsive velocity increment for each mission time, ΔV , in miles per second is plotted against the mission time in days for launch years of 1971 and 1980 in Figs 3 and 4, respectively. In all cases, the mission starts from an Earth parking orbit of 1.1 Earth radii, and at atmospheric braking is used at Earth return. The lowest periapsis of the Mars pass considered for the gravity and the propulsive-gravity-turn trajectories is 1.1 Mars radii. For references, the total ΔV required for a comparable direct lunar landing and return mission (5.3 mps) and the minimum ΔV for a one-way fly-by transfer to Mars (about 2.2 mps) are indicated on the ordinate.

Many of the Mars round trips require a ΔV substantially less than that for the lunar landing. The Mars trip times, however, are considerably longer than the lunar trip time, which is of the order of a week.

Gravity-turn trajectories are possible only at total trip times of approximately 1 year and again at trip times greater than about 1½ years. If 1980 is the launch year, the lowest ΔV for a gravity turn occurs for a trip time of 540 days.

By admitting the use of thrusting near Mars, the propulsive-gravity-turn type of trajectory, round trips become possible

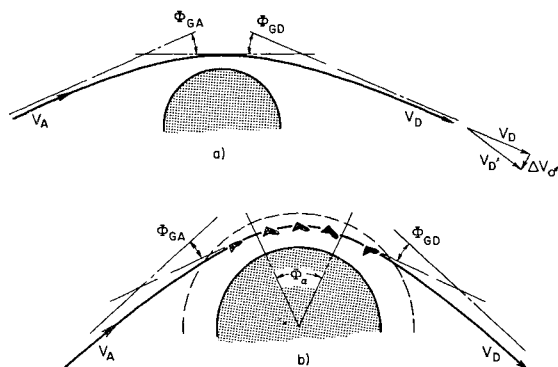


Fig 2 Types of nonstop round-trip trajectories: a) gravity turn and propulsive-gravity turn; b) atmospheric turn

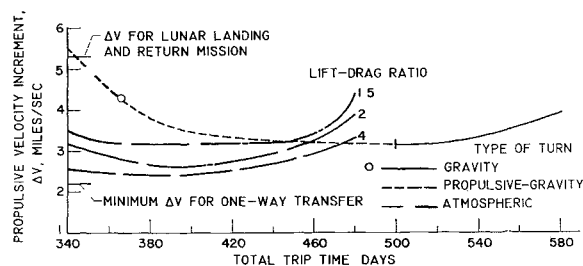


Fig 3 Round-trip nonstop missions in 1971

over a wide range of trip times. For 1980, the minimum ΔV is slightly less than that for the best gravity turn and occurs at a shorter trip time, about 500 days. Also, in both 1971 and 1980, there is only a slow increase in ΔV with decreasing trip time for trip times down to about 400 days.

Even further reductions in ΔV occur when an aerodynamic turn is used at Mars. Values only slightly greater than that for a one-way transfer occur for a vehicle with a lift-drag ratio of 4. Significant reductions in ΔV below that for the propulsive-gravity turn exist also for the more practical lift-drag values of 1.5 and 2.0. The trip times for low ΔV are between about 380 and 420 days for this case.

The effect of launch year on the required ΔV may be seen by comparing the values in Figs 3 and 4. For the gravity and the propulsive-gravity turns, the values of ΔV are greater in 1980 than in 1971. This effect is due to the eccentricity of the Mars orbit. The trips in 1971 pass Mars when Mars is near its perihelion, as illustrated in Fig 1. The trips in 1980, however, pass Mars when Mars is near its aphelion. A comparison of the atmospheric turns in 1971 and 1980 shows that the required propulsive velocity increment for this type of trajectory is least sensitive to the launch year.

Several factors not discussed in this note are also important in the case of atmospheric turns: g loads, heat loads, and feasible lift-drag ratios. In most cases, the g loads during the atmospheric turns are less than 10 Earth g 's, which is about the limit of human tolerance. The vehicle must be capable of absorbing both the heat load associated with the aerodynamic turn at Mars and the Earth atmospheric entry. The lowest ΔV available will depend on the practically realizable lift-drag ratios, which may be of the order of 2.0. The heat loads also depend on the vehicle lift-drag ratio. The atmospheric-turn trajectories pose challenging but not unfeasible aerodynamic and heat-protection problems, which require further study.

Conclusions

The following conclusions can be drawn from the present study of Mars nonstop round-trip trajectories using gravity, propulsive-gravity, and atmospheric turns at Mars:

1) When compared with gravity turns, the use of small amounts of propulsion near Mars markedly expands the range

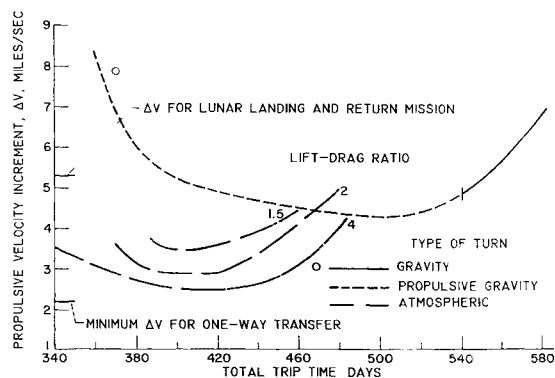


Fig 4 Round-trip nonstop missions in 1980

of possible trip times and in some cases reduces the required propulsive velocity increment

2) The use of an atmospheric turn at Mars can reduce the required propulsive velocity increment to a value approaching that for a one-way transfer to Mars, depending on the feasible vehicle lift-drag ratios. Low propulsive velocity increments occur for trip times down to about 1 year.

3) In general, greater propulsive velocity increments are required in 1980 than in 1971. The propulsive velocity increments for the atmospheric-turn trajectories are the least affected by the launch year.

4) The propulsive-gravity and the atmospheric-turn trajectories appear to offer the potential of fast, light-weight, nonstop round trips to Mars.

Reference

¹ Knip, G., Jr. and Zola, C. L., "Three dimensional trajectory analysis for round-trip missions to Mars," NASA TN D-1316 (1962).

Nonlinear Pressure Coupling in Cylindrical Shell Analysis

PAUL E. WILSON* AND EDWARD E. SPIER†

General Dynamics/Astronautics, San Diego, Calif

Nomenclature

- a = radius of shell middle surface
- A, B = constants of integration
- D = flexural rigidity, $Eh^3/12(1 - \nu^2)$
- E = modulus of elasticity
- h = shell thickness
- i = $(-1)^{1/2}$
- k = shell parameter, Eh/a^2
- m = nondimensional load parameter
- M_0, Q_0 = moment and shear at discontinuity neglecting $N_x(d^2w/dx^2)$
- M_N, Q_N = moment and shear at discontinuity including $N_x(d^2w/dx^2)$
- N_x = axial stress resultant, positive when tensile
- p = internal pressure
- w = radial deflection measured positive inward
- w, w_p = complementary and particular solutions, respectively
- x = axial coordinate
- α, β, γ = parameters entering into complementary solution
- δ_1, δ_2 = membrane expansions given by Eq. (7)
- η = shell thickness ratio, h_1/h_2
- λ^4 = shell parameter, $k/4D$
- ν = Poisson's ratio

Introduction

MANY structural problems in the aerospace industry involve highly pressurized shells with large radius-thickness ratios, and under these circumstances, as suggested by Hetenyi,¹ the coupling effects of pressure often have a significant influence on discontinuity shears, moments, and stresses. Accordingly, a number of investigations have recently been focused on this problem for pressurized cylindrical,²⁻³ spherical,^{9,10} and arbitrary shells of revolution.¹¹ For internally pressurized shells, comparisons made between

Received October 30, 1963. This note summarizes results of one phase of research that was sponsored by General Dynamics/Astronautics under Research Program No. 111-9372. The authors extend their appreciation to D. R. Cropper and others at General Dynamics/Astronautics for assisting in the preparation of this note.

* Design Specialist, Structures Research Group.

† Design Specialist, Structures Research Group. Member AIAA.

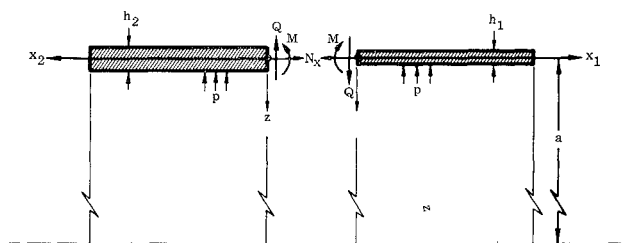


Fig 1 Shell juncture

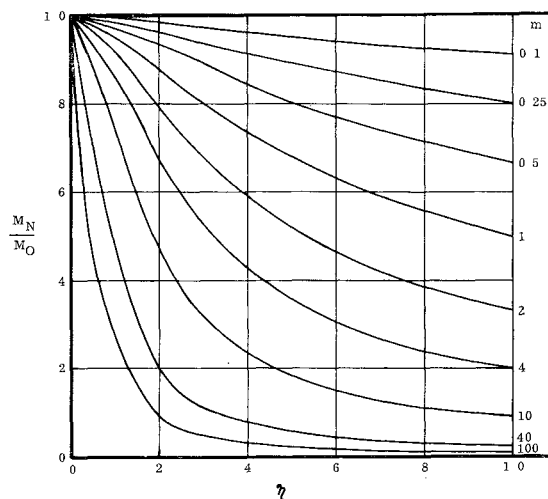


Fig 2 Moment comparison curves

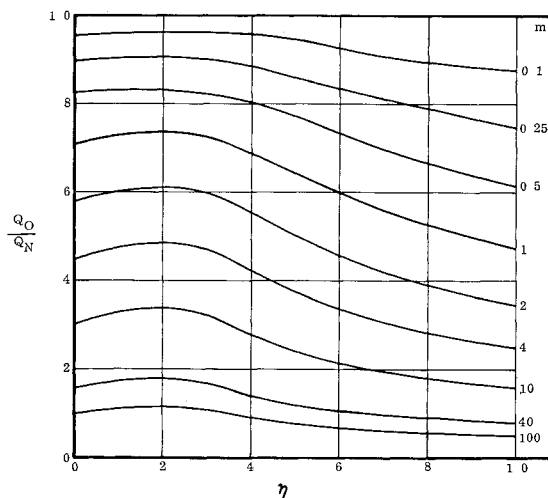


Fig 3 Shear comparison curves

discontinuity analyses that include and neglect the coupling effects of meridional load^{7,8} imply that use of the refined method generally yields lower calculated maximum stresses and results in a lighter-weight structure.

In this note, two well-known thin shell theories are used to evaluate and compare shears and moments at the juncture of two pressurized cylindrical shells. For highly pressurized cylinders with large radius-thickness ratios, the numerical results indicate that nonlinear coupling effects of pressure significantly influence computed values of discontinuity shears and moments.

Theory

The differential equation that governs small axisymmetric displacements of thin cylindrical shells may be written in the form¹²

$$D \frac{d^4 w}{dx^4} - N_x \frac{d^2 w}{dx^2} + \frac{Eh}{a^2} w = -p + \nu \frac{N_x}{a} \quad (1)$$